Heat resilience in embryonic zebrafish revealed by an *in vivo* stress granule reporter

Ruiqi Wang[1], Hefei Zhang[1,2], Jiulin Du[1,2], Jin Xu[1*,#]

[1]Institute of Neuroscience, State Key Laboratory of Neuroscience, Shanghai Institutes for Biological Sciences, Chinese Academy of Sciences, Shanghai 200031, China. [2]CAS Center for Excellence in Brain Science and Intelligence Technology, Shanghai 200031, China.

*: Correspondence should be addressed to:

Jin Xu, Ph.D.

jin.xu@ion.ac.cn

+862154921818

320 Yue Yang Road, Shanghai, China, 200031

#: Current address:

Jin Xu, Ph.D.

Department of Neuroscience, Baylor College of Medicine

Jan and Dan Duncan Neurological Research Institute at Texas Children's Hospital

1250 Moursund St, Houston, TX 77030

832-824-8118

jin.xu@bcm.edu

JCS Advance Online Article. Posted on 26 September 2019

Abstract

Although the regulation of stress granules has become an intensely studied topic, current investigations of stress granule assembly, disassembly and dynamics are mainly performed in cultured cells. Here we report the establishment of a stress granule reporter to facilitate the real-time study of stress granules *in vivo*. Using CRISPR/Cas9, we fused a green fluorescence protein (GFP) to the endogenous G3BP1 in zebrafish. The GFP-G3BP1 reporter faithfully and robustly responded to heat stress in zebrafish embryos and larvae. The induction of stress granules varied by brain regions under the same stress condition, with the midbrain cells showing the highest efficiency and dynamics. Furthermore, preconditioning using lower heat stress significantly limited stress granule formation during subsequent heat stress. More interestingly, the stress granule formation was much more robust in zebrafish embryos than in larvae and coincided with significant elevated phosphorylated eIF2α and enhanced heat resilience. Therefore, these findings have generated new insights into stress response in zebrafish during early development and demonstrated that the GFP-G3BP1 knockin zebrafish could be a valuable tool for the investigation of stress granule biology.

Keywords: Stress granule, G3BP1, *in vivo* reporter, Zebrafish, heat shock, stress resilience, early development

Introduction

Stress granules are cytoplasmic structures rich in mRNA and RNA-binding proteins. They are usually formed when translation initiation is inhibited. The inhibition could be caused by certain drugs, altered expression or modification of translation initiation factors, or dissociation of ribosomal-mRNA (Buchan and Parker, 2009; Dang et al., 2006; Gilks et al., 2004; Kedersha et al., 2000; Mokas et al., 2009). Furthermore, as the name suggests, stress granules are induced upon various stress insults, such as heat shock, viral infection and increased oxidative or endoplasmic reticulum (ER) stress (Kedersha et al., 1999; Nover et al., 1989; Protter and Parker, 2016; White and Lloyd, 2012; Wolozin, 2012). Hence, the formation of stress granules is considered as a protective cellular mechanism for resource conservation and survival under unfavorable conditions, and is characterized by the translation inhibition of most house-keeping genes and the preferential translation of pro-survival stress-responsive genes (Anderson and Kedersha, 2002; Kedersha et al., 2013; McCormick and Khaperskyy, 2017).

Stress granule formation is a dynamic process, with its assembly and disassembly regulated by the abundance of many RNA-binding proteins (Protter and Parker, 2016). Mounting evidence indicates that stress granule dysregulation could contribute to the development of some neurodegenerative diseases (Apicco et al., 2018; Ash et al., 2014; Li et al., 2013; Maziuk et al., 2017; Xu et al., 2019) and chemoresistance in cancer cells (Anderson et al., 2015). Recently, we have shown that stress granule is also regulated by circadian rhythm (Wang et al., 2019). Therefore, stress granules play important roles in human health and diseases and warrant in depth investigation.

Most studies of stress granules have been performed in cultured cells by immunolabeling stress granule marker proteins in fixed cells, or by live imaging of fluorescent protein-tagged stress granule markers (Kedersha and Anderson, 2007; Kedersha et al., 2000; Kedersha et al., 2005; Kedersha et al., 2008). *In vivo* studies of stress granules have been attempted using fixed tissues by immuneflouresence labeling (Bai et al., 2016; Shelkovnikova et al., 2017; Wang et al., 2019). However, the spatial and temporal regulation of the stress granules and their dynamics under physiological or disease states are entirely unknown. A previous study

using fluorescence-tagged RNA as a reporter has generated some clues on the RNA dynamics in *Drosophila* muscle cells(van der Laan et al., 2012). Nevertheless, the current knowledge about the dynamics of protein components in stress granules *in vivo* is absent.

Ras GTPase-activating protein-binding protein 1 (G3BP1) is one of the RNA-binding proteins that could initiate and promote stress granule formation(Tourriere et al., 2003) . By binding untranslated mRNA and serving as a scaffolding protein, G3BP1 could facilitate the recruitment of other stress granule components via aggregation-prone low complexity domains(Buchan, 2014; Mahboubi and Stochaj, 2017). G3BP1 has been commonly used as a stress granule marker protein(Mahboubi and Stochaj, 2017; Protter and Parker, 2016) and green fluorescent protein (GFP)-tagged G3BP1 is routinely used to study stress granule dynamics in live cells. However, as overexpression of G3BP1 could induce stress granules(Anderson and Kedersha, 2008; Mahboubi and Stochaj, 2017), monitoring stress granule with overexpressed protein is not an ideal approach. Previously, we have established a knockin cell line expressing GFP-G3BP1 under the endogenous G3BP1 promoter (Wang et al., 2019). In the current study, we successfully tagged the endogenous zebrafish G3BP1 with GFP using CRISPR-Cas9 gene editing and validated it to be a functional *in vivo* stress granule reporter. Furthermore, with this new tool, we have found that the efficiency and dynamics of stress granule formation differed in various brain regions, and that heat stress pre-conditioning blunted stress granule formation *in vivo*. Surprisingly, we have also found higher stress resilience in zebrafish embryos during early development. Therefore, we have demonstrated that this novel knockin GFP-G3BP1 reporter could be a highly useful tool to investigate stress granule regulation *in vivo*.

Results

Establishment and characterization of an *in vivo* stress granule reporter

We reasoned that the ideal *in vivo* reporter of stress granule should have the following properties. First, the marker protein should be functionally conserved in various species. Second, the expression of reporter protein would not interfere with the physiological formation of stress granules. Third, the stress granules could be easily monitored in real-time, and the dynamics could be analyzed. Given that zebrafish (*Danio Rerio*) has become a valuable tool in biological research to visualize physiological changes using live imaging due to its transparent body at embryonic and early larval stages (Cooper et al., 1999a; Cooper et al., 1999b; Kimmel, 1989; Kimmel and Warga, 1988; Solnica-Krezel et al., 1995; Spitsbergen and Kent, 2003), we decided to genetically knock in a GFP tag to the zebrafish G3BP1, which shares 65% protein sequence homology with its human counterpart. With this approach, the expression of GFP-tagged G3BP1 will be under the control of endogenous G3BP1 gene promoter, and the stress granule formation will not be affected by G3BP1 overexpression. Although stress granules biology has not been well characterized in zebrafish, several studies have shown the formation of cytosolic granules resembling stress granules either under stress or with the expression of neurotoxic, stress granule-inducing proteins(Bosco et al., 2010; Zampedri et al., 2016).

To perform gene editing in zebrafish, we microinjected the sgRNA and Cas9 nuclease into the zebrafish embryos to excise the zebrafish G3BP1 gene within a 250-bp region covering either the start codon or the stop codon and then attempted to fuse the GFP sequences next to the N or C terminus of zebrafish G3BP1 via recombination of the donor DNAs. The donor DNA was generated by PCR and contained a GFP fragment flanking two 35-bp homologous arms. This strategy has been shown to promote recombination efficiency (Paix et al., 2017). However, we were unable to fuse the GFP immediately adjacent to either the start or stop codons after numerous attempts. Therefore, we modified the strategy and directly introduced the donor DNA at the excision cite nearest to the N-terminus (Fig. 1A), and were able to obtain zebrafish expressing endogenous G3BP1 with GFP inserted after the 10^{th} residue at the N-terminus (Fig. 1B, Fig. S1A). The first 10 residues in G3BP1 are highly conserved but not

required for its function as a stress granule regulator (Vognsen et al., 2011; Vognsen et al., 2013). To validate that the insertion of GFP between the 10th and 11th residues of G3BP1 will not impair its function, we made two GFP-G3BP1 fusion constructs, one with GFP immediately after ATG start codon (0AA-GFP-G3BP1) and the other with GFP inserted between the 10th and 11th residues (10AA-GFP-G3BP1). We compared the stress granule formation (Fig. S1B, C, E, F) and dynamics (Fig. S1D, G) in cells transiently transfected with either of those two stress granule reporters and used heat shock (Fig. S1B, C, D) or sodium arsenite Fig. S1E, F, G) to induce stress granule formation. There was no significant difference in the response patterns between the two constructs. Furthermore, we performed whole genome sequencing of the F1 10AAGFP-G3BP1 knockin fish to examine whether GFP could be erroneously inserted in other genes, and we found that G3BP1 was the only gene tagged, indicating that the GFP-reporter was unique to G3BP1 (see methods). Therefore, we proceeded to use the 10AA-GFP-G3BP1(denoted as GFP-G3BP1 thereafter) knockin zebrafish in our subsequent studies.

We first characterized the expression patterns of GFP-G3BP1. Under normal basal condition, GFP-G3BP1 was diffusely expressed in cytosol. Ten minutes of heat shock significantly increased granule formation in the lens, retina and brain. After removing stress, the granules quickly disappeared (Fig. 1 C). The distribution and aggregation patterns of zebrafish GFP-G3BP1 reporter was identical to those of cellular stress granule reporters (Tourriere et al., 2003; Wang et al., 2019) and indicated that we have successfully established an *in vivo* stress granule reporter.

Next, we evaluated whether GFP-G3BP1 reporter could respond to other stress signals. Sodium arsenite (SA) is a potent stress granule-inducing agent (Matsuki et al., 2013; Parker et al., 1996; Tourriere et al., 2003) and dithiothreitol (DTT) is commonly used to induce ER stress (Lodish and Kong, 1993; Shen et al., 2002). We treated 1dpf zebrafish with SA or DTT for 30 to 60 minutes and assessed the stress granule formation by immunofluorescence microscopy (Fig. 2B, C). The fish embryo could sustain 30 mM SA treatment up to 40 minutes. Longer treatment (50 minutes) would significantly damage the integrity of the epidermis and cause

cardiac arrest (data not shown). SA was able to induce stress granules in the retina and moderately in epidermis (data not shown) but not in the brain (Fig. 2A, B). Exposure of 20 mM of DTT for up to 60 minutes did not affect the epidermis integrity and induced the formation of stress granules in the epidermis in both the eye and midbrain regions (Fig. 2 C). Therefore, the *in vivo* GFP-G3BP1 reporter could respond to known stress granule-inducing agents.

Dissociation of ribosome-mRNA with puromycin could stimulate stress granule formation, while blocking the elongation of ribosome by cycloheximide could suppress stress granule(Kedersha et al., 2000). To further characterize GFP-G3BP1 as an *in vivo* stress granule marker, we treated the GFP-G3BP1 KI zebrafish with puromycin and found increased GFP-G3BP1-positive punctate in the epidermal cells in the eyes and midbrain (Fig. 2 D). In contrast, cycloheximide treatment could block the formation of stress granule in the midbrain cells of fish exposed to heat stress (Fig. 2 E). Taken together, these results validated the endogenous GFP-G3BP1 as a reliable *in vivo* marker of stress granule.

Stress granule formation differs by brain regions

Once we validated the reliability of GFP-G3BP1 reporter *in vivo*, we investigated whether the stress response could vary by different brain regions during development. Zebrafish brain morphogenesis starts after the closure of neural tube, usually at 17 hpf (Kimmel et al., 1995; Lowery and Sive, 2005). By 1pf, the indentations at the outside of the neural tube could clearly define fore-, mid- and hindbrain(Kimmel et al., 1995; Lowery and Sive, 2005). We examined the stress granule formed in brain cells in those regions under the identical condition (Fig. S2). 1dpf zebrafish were exposed to 42^{o}C heat stress for 10 minutes, and the brain cells at 20 μm under epidermis were imaged and assessed for the number of stress granules (Fig. 3 A). Interestingly, the number of stress granules in the midbrain cells was significantly higher than that in either the forebrain or hindbrain (Fig. 3B). This difference was unlikely to be caused by the different GFP-G3BP1 expression levels (Fig. S2).

With the GFP-G3BP1 reporter, we were able to assess stress granule dynamics *in vivo* using fluorescence recovery after photobleaching (FRAP). Although FRAP of a stress granule

component protein is a common approach for stress granule characterization, this method has never been attempted in live animals. We compared the stress granules in the midbrain and hindbrain cells at same depth under epidermis and found the stress granule dynamics and mobile fraction were higher in the midbrain cells (Fig. 3 D, E), consistent with higher number of granules in those cells after heat stress. It is worth noting that comparing to stress granules formed in cultured cells (Wang et al., 2019; Wheeler et al., 2016), the dynamics of stress granules in embryonic stage zebrafish brain cells were much lower. After photobleaching, the fluorescence recovery could only reach 30% of the original signal intensity after 80 seconds (Fig. 3.D), indicating moderate dynamics.

Stress sensitivity and resilience in zebrafish embryos

It has been shown that chronic or preconditioning stress could limit stress granule assembly under subsequent acute stress in cultured neurons (Shelkovnikova et al., 2017). To determine the effect of preconditioning stress on stress granule *in vivo*, we first exposed 1dpf zebrafish to 35 ^{o}C for 6 hours. Unlike short exposure (10 minutes) at 42 ^{o}C, 35 ^{o}C treatment did not induce any stress granule in midbrain cells or retina (Fig.4 A). Consistent with the observation in cultured cells, 35^{o}C preconditioning significantly reduced the stress granule formation at 42 ^{o}C (Fig.4. A, B). Therefore, chronic heat stress could diminish the fast formation of stress granule during heat shock *in vivo*.

The *in vivo* stress granule reporter is also a great tool to determine whether stress granule formation could be affected by the age of zebrafish during development. We heat shocked (42 ^{o}C) GFP-G3BP1 knockin zebrafish of different age (1, 2, 3, and 11 dpf) for 20 minutes and analyzed the stress granule formation in the midbrain cells by live imaging. Surprisingly, the efficiency of stress granule formation was much more efficient in 1dpf embryo and gradually decreased with developmental age (Fig. 5A, B, Fig. S3). At 8 minutes with heat shock, granules in 1dpf fish were clearly visible and their number consistently increased with the duration of heat shock. In contrast, for 3 and 11dpf fish larvae, only a few granules per 100 cells were detected even after 12 to 20 minutes heat shock. Therefore, the zebrafish in embryonic stage has a more efficient stress response.

To gain mechanistic insight into the differential regulation of stress granules in fish at different developmental stages, we examined the expression of phosphorylated and total eIF2α in the midbrain. The relative abundance of phosphorylated (p) and total (t) eIF2α is a determining factor in the stress granule formation, with higher ratio of p-eIF2α to t-eIF2α leading to translation suppression and granule assembly(Anderson and Kedersha, 2002; Wang et al., 2019). In the absence of heat stress, the expression level of t-eIF2 α in the midbrain tissues of 1 and 3 dpf zebrafish embryos were almost 15 times of that in 11 dpf larvae, with minimal p- eIF2α (Fig.6. A, B). With 10-minute heat shock, the p-eIF2α in 1dpf fish embryo increased dramatically (Fig.6. A, C, D). This change most likely contributed to the abundant stress granules in 1dpf fish during heat stress (Fig. 5). It is noted that in 3-dpf fish, the level of t-eIF2α was marginally higher than that in 1 dpf fish, while the level of p-eIF2α was much lower (Fig. 6C).

The formation of stress granule is a cellular protective mechanism during acute stress(Buchan and Parker, 2009). We have noticed that the heat tolerance capacity was much lower in 11 dpf larvae than in the 1 dpf embryo, demonstrated by increased incidents of cardiac arrest under heat stress (data not shown). To confirm this observation at cellular level, we performed TUNEL labeling of the epidermal cells (Fig.6 E, Fig. S4). The TUNEL signals were reverse correlated with the abundance of stress granules in the skin cells, with significant TUNEL positive signals in 11 dpf fish. We were unable to assess TUNEL signals in the midbrain cells due to poor reagent penetration (data not shown). Therefore, using the *in vivo* GFP-G3BP1 knockin stress granule reporter fish, we have found higher heat stress resistance in zebrafish embryo than in larvae, correlated with more robust stress granule formation and significantly higher expression of p-eIF2α in embryonic stage

Discussion

In this study we have established a novel *in vivo* stress granule reporter in zebrafish. This tool has the potential to elevate stress granule investigation to a new level to better understand the regulation of stress granules by various conditions. Via this new reporter, we could track the dynamic change of stress granules *in vivo* in different parts of the body in real time and uncover interesting biological phenomenon.

As the assembly and disassembly of stress granule is a dynamic process highly affected by the abundance of stress granule components via liquid-liquid phase separation (Molliex A, Cell 2016), reliable markers that can faithfully and efficiently trace the change of stress granules are essential. In most if not all the studies of stress granules dynamics in cultured cells, worms or flies using live imaging, overexpression of fluorescence-tagged stress granule components is the standard practice (Kedersha and Anderson, 2007; Kedersha et al., 2008; Martin and Tazi, 2014). To achieve robust signals, cells or flies stably expressing aggregate-prone, disease-associated stress granule residents such as Fus and TDP-43 have also been used to visualize stress granules(De Graeve et al., 2019; Marrone et al., 2018). However, one clear drawback of this approach is that the overexpression of those stress granules marker proteins, including G3BP1, could artificially promote stress granule formation as they are frequently nucleating proteins facilitating the assembly of stress granules (Tsai et al., 2016). By contrast, GFP-tagged endogenous G3BP1 would faithfully reflect the transcription, translation of G3BP1 and the assembly and disassembly of stress granules. With this new tool, we have made some observations that could not be achieved previously. One obvious advantage of this system is that we could observe stress granule dynamics using FRAP in live animals in various parts of the body. In this study, we have provided one example where real-time stress granule dynamics could be monitored in different brain regions after heat shock.

A surprising observation from our study is the heat stress resilience at the embryonic stage in zebrafish. In mammals, heat shock during early embryonic development usually results in deleterious consequences(Alderman et al., 2018; Edwards et al., 1997; Icoglu Aksakal and

Ciltas, 2018; Menon and Nair, 2018). Heat resilience is gradually increased with development and coincided with the expression of heat shock proteins (Edwards et al., 1997; Mishra et al., 2018; Walsh et al., 1997). Contrary to our initial expectation, we found that 1dpf embryo could form stress granules much more efficiently than the larvae and is more resistant to heat stress. This phenomenon coincided with significant increase of phosphorylated eIF2α and the absence of cell death. Previous studies have implicated the roles of corticotropin-releasing factor and heat shock proteins in the stress resistance in zebrafish during development (Alderman et al., 2018; Mishra et al., 2018). Our study has now demonstrated the involvement of eIF2α-stress granule in the stress response in early development. While post-hatching larvae and juveniles could escape from unfavorable stress, for immobile zebrafish embryos, an efficient stress response mechanism would be vital for survival.

It is also of interest to find decreased stress granule formation in zebrafish preconditioned by chronic heat stress. Chronic ER stress due to abnormal proteasome and lysosomal degradation pathway is a feature of aging and neurodegeneration (Hetz and Saxena, 2017; Naidoo, 2009; Oakes and Papa, 2015; Shelkovnikova et al., 2017). Our *in vivo* results validated similar observation from cultured cell(Shelkovnikova et al., 2017), and suggested that chronic stress could weaken a cellular defense mechanism and render cells vulnerable to acute stress, such as viral infection.

Although our proof-of-concept study has demonstrated the usefulness of this *in vivo* GFP-G3BP1 reporter, the system is limited by the time window of live imaging only during embryonic, larval and juvenile stages. Long term age-related study will not be feasible due to the change of zebrafish anatomy. Nevertheless, the effects of various disease-related proteins, especially those encoded by genes with pathogenic mutations, on stress granule biology *in vivo* could still be assessed using this model via genetic manipulation. We recognize that even though this *in vivo* GFP-G3BP1 reporter could respond to several forms of stress, the sensitivity apparently varied greatly. While our reporter is responsive to 30 mM sodium arsenite, others have shown previously that lower concentrations cause developmental defects and can even be

lethal(Fuse et al., 2016; McCollum et al., 2014). Heat stress was much more efficient to induce the formation of GFP-positive stress granules, and would be the more suitable background stress source for identifying enhancers and suppressors of stress granule formation. Although we have tested a few stress paradigms, it will be of great interest to use this system to evaluate the involvement of stress granules and their real-time regulation in animal exposed to various additional environmental and behavioral stress. By demonstrating the value of *in vivo* stress granule markers in zebrafish, we could envision the establishment of additional *in vivo* stress granule markers using similar approach in various organisms, such as in *C. elegans*. With the development and optimization of these tools, we could have a more comprehensive understanding of the regulation and function of stress granules in adaptation, stress tolerance, survival and its relevance to human diseases.

MATERIALS AND METHODS

MATERIALS

Zebrafish

Adult zebrafish (Danio rerio) were maintained in the National Zebrafish Resources of China (Shanghai, China) with automatic fish housing system (ESEN, China) at 28°C following the standard protocol(Mu et al., 2012). Embryos were raised under a 14h-10h light-dark cycle in E2 medium (15 mM NaCl, 0.5 mM KCl, 2.7 mM $CaCl_2$, 1 mM $MgSO_4$, 0.7 mM $NaHCO_3$, 0.15 mM KH_2PO_4, 0.05 mM Na_2HPO_4). Zebrafish-handling procedures were approved by Institute of Neuroscience, Shanghai Institutes for Biological Sciences, Chinese Academy of Sciences.

Cell culture

SH-SY5Y cells were obtained from American Type Culture Collection (ATCC, VA, USA) and

cultured at 37°C in 5% CO2 in Dulbecco's modified Eagle's medium (Invitrogen), supplemented with 10% fetal bovine serum (Invitrogen) and antibiotics (Penicillin and streptomycin, HyClone, SV30010). Cells were confirmed free of mycobacteria.

METHODS

Generation of GFP-G3BP1 Knock-in Zebrafish Mediated by CRISPR/Cas9

CRISPR/Cas9-based gene editing techniques were used to generate GFP-G3BP1 knockin Zebrafish (Li et al., 2015; Paix et al., 2017). The sequences of sgRNAs were designed according to previously reported criteria(Chang et al., 2013), and sequences GCCAAGTGCCCAGCTTGTC were selected as sgRNAs target in the zebrafish G3BP1 gene. The T7 promoter-sgRNA DNA template was constructed by annealing three pairs of oligonucleotides each with sticky ends using T4 ligase. The forward and reverse sequences for 3 pairs of oligos are:

F1: GAATTTAATACGACTCACTATAGCCAAGTGCCCAGCTTGTCGTTT

R1: GACAAGCTGGGCACTTGGCTATAGTGAGTCGTATTAAATTCC

F2: TAGAGCTAGAAATAGCAAGTTAAAATAAGGCTAGTCCGT

R2: GACTAGCCTTATTTTAACTTGCTATTTCTAGCTCTAAAAC

F3: TATCAACTTGAAAAAGTGGCACCGAGTCGGTGCTTTTT

R3: AAAAGCACCGACTCGGTGCCACTTTTTCAAGTTGATAACG

The sgRNAs were synthesized with the HiScribe™ T7 High Yield RNA Synthesis Kit (NEB : E2040S) and purified with the RNeasy Mini Kit (QIAGEN). The donor DNA construct contained GFP sequences flanked by two 35-bp homologous arms directing at the endogenous G3BP1 sequences. The donor DNA was constructed via PCR by PrimeSTAR® HS DNA Polymerase (Takara) and purified with the PCR Purification Kit (TIANGEN). Cas9 Nuclease (NEB : M0386S), sgRNAs and donor DNA were co-injected into the animal pole of zebrafish embryos at one-cell stage. Each embryo was injected with 1 nL solution containing 600 ng/μl Cas9 Nuclease and 30 ng/μl sgRNA and 300 ng/μl Donor. The embryos with fluorescence selected and were raised to adulthood. The correct transgene expression in F0 fish was validated by PCR amplification and sequencing. The forward and reverse sequences for PCR

identification.

f1: GGGTGAAGAAACAGTGGAGGTGC

f2: CGGCCCCGTGCTGCTGCCCGACAACC

r: CACCTGTGCAGGTAGTCAGGAGCCTGG

F0 GFP-G3BP1 knockin male fish was mated with albino (slc45a2^{b4}) fish to generate F1 offspring. Whole genome sequencing of F1 was performed by Annoroad Inc. to validate the absence of off-target insertion of GFP at locations other than at the intended site. Briefly, genomic DNA was isolated from pools of 3 3-mpf (months post-fertilization) F1 GFP-G3BP1 KI zebrafish. The GFP sequences and zebrafish genome (Danio Rerio) were designated as reference genome. Clean reads were mapped to reference genome by BWA (Burrows-Wheeler Alignment tool). Reads that could match to both the zebrafish genome and GFP were selected. Then the selected reads were re-aligned with Blast to map the specific genetic loci in zebrafish genome. The mapping results indicated that GFP was inserted between 25636639 and 25636640 on chromosome 14 in the G3BP1 gene.

Plasmid transfection

SH-SY5Y cells were transfected with GFP-G3BP1 plasmids using Lipofectamine 2000 reagent (Invitrogen) at 5 μg of DNA per 3.5-mm dish. Plasmids: 10AA-GFP-G3BP1 and 0AA-GFP-G3BP1 were generated by PCR cloning, with GFP sequences cloned after the 10th residue (10AA-GFP-G3BP1) or after the ATG start codon (0AA-GFP-G3BP1). Cells were harvested at 48 h for FRAP analysis.

Live imaging under the heat shock condition

For live imaging of stress granules, zebrafish at different age were individually embedded in 6 cm glass dish in 1.5% low melting-point agarose (Sigma) with ventral side facing up. For 1or 2 dpf zebrafish, the embryos were first dissected from eggs before embedding. Then heated embryo medium (15mM NaCl, 0.5mM KCl, 0. 05mM Na2HPO4, 0. 15mM KH2PO4, 1.0mM CaCl2, 1.0mM MgSO4, 0.7mM NaHCO3) was pumped continuously in and out of the dish

with a peristaltic pump. Medium within the dish would reach 42°C within 30 seconds. Time lapse and Z-stack images were taken at indicated conditions with a confocal microscope (Nikon NiE) with 25X water immersion-lens. The resolution of all the images was 1024 × 1024 pixel**.**

Drug treatment

1dpf zebrafish were dissected from the eggs and then were soaked into drug solution for indicated amount of time (between 30-60 minutes). Subsequently, the embryos were fixed with 4% paraformaldehyde for 24h and then transferred to PBS for imaging. The concentrations of Sodium Arsenite (S7400-100G, Sigma) and DTT (Sigma) and Puromycin (A11138, Sigma) were 30 mM and 20 mM and 10mg/ml, respectively. For Cyclohexamide experiment, 1dpf zebrafish was treated with 1mg/mL CHX for 1h then 42°C heat shock with the exist of CHX for 10min then fixed with 4% PFA for 24h for imaging.

Fluorescence recovery after photo bleaching (FRAP).

For FRAP experiment in zebrafish, 1hpf zebrafish were first dissected from the eggs. The embryos were soaked into 42°C embryo medium and embedded in 6 cm glass dish in 1.5% low melting-point agarose (Sigma) with ventral side up. Stress granules were photobleached and GFP intensity was measured before and after bleaching.

For FRAP experiment in SH-SY5Y cells, cells were transfected with GFP-G3BP1 reporter plasmids. After another 48 h, cells were treated with 20μM Sodium Arsenite for 30 minutes to induce stress granules. Stress granules were photobleached and GFP intensity was measured before and after bleaching as describe(Wang et al., 2019)

Pre-conditioning heat stress

For pre-conditioning heat stress, 1dpf zebrafish embryos was raised at basal temperature is 28°C then were removed from eggs and soaked in 35°C embryo medium for 6h, and then transferred to 42°C embryo medium for 10min. Subsequently, the heat shocked embryos were fixed in 4% paraformaldehyde for 24h and then transferred to PBS for imaging.

Confocal imaging

Time lapse and Z-stack images were taken at indicated condition. Images were taken with confocal microscope Nikon NiE-A1 with 25X water immersion-lens or Nikon FN1 with 60X water immersion-lens (for FRAP). The resolution of all the images was 1024 × 1024 pixel.

Western blotting

Zebrafish embryos and larvae were incubated at 42°C for 10min, and the midbrain tissues were dissected and lysed in RIPA buffer (150mM NaCl, 50mM Tris pH8.0 , 1% NP40, 1% sodium deoxycholate, 0.1%SDS) supplemented with protease inhibitor cocktail (Roche) and phosphatase inhibitor cocktail (Roche). Proteins were resolved by SDS-PAGE, and the protein bands were visualized using Bio-Rad western ECL substrate kit. The band intensity in immunoblots was determined by Bio-Rad Quantity One software. The primary antibodies used are: Mouse anti-eIF2α (sc-133132 Santa Cruz Biotechnology, 1:1,000); Rabbit anti-phospho-eIF2α (9721 Cell Signaling Technology, 1:1,000); Mouse anti-Actin (M20010, Abmart, 1:5,000).

TUNEL assay

Zebrafish at different age were heat shocked for 20min then were fixed in fresh 4% paraformaldehyde in PBS overnight at 4°C and dehydrated using methanol (3× 10min). Zebrafish were further permeabilized in a solution containing 0.1% Triton X-100 and 0.1% sodium citrate in PBS for 1h at room temperature followed by rinses in PBS (2× 10min). The samples were subjected to TUNEL assay using the TMR-RED *in situ* cell death detection kit (Roche, Basel, Switzerland) according to the manufacturer's protocols, and then rinsed in PBST (PBS, 0.3% Tween) (3× 15min). Samples were also stained with DAPI for 10 min with rinses in PBST (2× 10min) to label nucleus. Images were taken with a confocal microscope (Nikon NiE) with 25X water immersion-lens.

Quantification and statistical analysis

The number of zebrafishes used in each experiment was described in figure legends. For data analysis, the results were presented as the mean ±S.E.M., with statistical significance analyzed using Student's t test or 2-way ANOVA by GraphPad, Prism 5. The choices of statistical test for each experiment was indicated in figure legends (* $P \leq 0.05$; ** $P \leq 0.01$; ***$P \leq 0.001$; ****$P \leq 0.0001$)

Acknowledgments

We thank Dr. Qian Hu for technical assistance in microscopy and imaging. This work was supported by State Key Laboratory of Neuroscience and National Natural Science Foundation of China grant (81771425) to J.X.

Author Contributions

J.X. conceived the idea, designed experiments, supervised the project and wrote the manuscript. H.Z. performed microinjection, selected knockin animals and conducted analysis under the supervision of J.D.. R.W. performed all the rest of the experiments and wrote part of the manuscript.

Declaration of Interests

J.X, R.W., H.Z., and J.D. are co-inventors on the patent application “The method for the establishment of a zebrafish model for stress granule research and its use” Application number CN2019102240623

References

Alderman, S. L., Leishman, E. M., Fuzzen, M. L. M. and Bernier, N. J. (2018). Corticotropin-releasing factor regulates caspase-3 and may protect developing zebrafish from stress-induced apoptosis. *Gen Comp Endocrinol* **265**, 207-213.

Anderson, P. and Kedersha, N. (2002). Visibly stressed: the role of eIF2, TIA-1, and stress granules in protein translation. *Cell Stress Chaperones* **7**, 213-21.

Anderson, P. and Kedersha, N. (2008). Stress granules: the Tao of RNA triage. *Trends Biochem Sci* **33**, 141-50.

Anderson, P., Kedersha, N. and Ivanov, P. (2015). Stress granules, P-bodies and cancer. *Biochim Biophys Acta* **1849**, 861-70.

Apicco, D. J., Ash, P. E. A., Maziuk, B., LeBlang, C., Medalla, M., Al Abdullatif, A., Ferragud, A., Botelho, E., Ballance, H. I., Dhawan, U. et al. (2018). Reducing the RNA binding protein TIA1 protects against tau-mediated neurodegeneration in vivo. *Nat Neurosci* **21**, 72-80.

Ash, P. E., Vanderweyde, T. E., Youmans, K. L., Apicco, D. J. and Wolozin, B. (2014). Pathological stress granules in Alzheimer's disease. *Brain Res* **1584**, 52-8.

Bai, Y., Dong, Z., Shang, Q., Zhao, H., Wang, L., Guo, C., Gao, F., Zhang, L. and Wang, Q. (2016). Pdcd4 Is Involved in the Formation of Stress Granule in Response to Oxidized Low-Density Lipoprotein or High-Fat Diet. *PLoS One* **11**, e0159568.

Bosco, D. A., Lemay, N., Ko, H. K., Zhou, H., Burke, C., Kwiatkowski, T. J., Jr., Sapp, P., McKenna-Yasek, D., Brown, R. H., Jr. and Hayward, L. J. (2010). Mutant FUS proteins that cause amyotrophic

lateral sclerosis incorporate into stress granules. *Hum Mol Genet* **19**, 4160-75.

Buchan, J. R. (2014). mRNP granules. Assembly, function, and connections with disease. *RNA Biol* **11**, 1019-30.

Buchan, J. R. and Parker, R. (2009). Eukaryotic stress granules: the ins and outs of translation. *Mol Cell* **36**, 932-41.

Chang, N., Sun, C., Gao, L., Zhu, D., Xu, X., Zhu, X., Xiong, J. W. and Xi, J. J. (2013). Genome editing with RNA-guided Cas9 nuclease in zebrafish embryos. *Cell Res* **23**, 465-72.

Cooper, M. S., D'Amico, L. A. and Henry, C. A. (1999a). Analyzing morphogenetic cell behaviors in vitally stained zebrafish embryos. *Methods Mol Biol* **122**, 185-204.

Cooper, M. S., D'Amico, L. A. and Henry, C. A. (1999b). Confocal microscopic analysis of morphogenetic movements. *Methods Cell Biol* **59**, 179-204.

Dang, Y., Kedersha, N., Low, W. K., Romo, D., Gorospe, M., Kaufman, R., Anderson, P. and Liu, J. O. (2006). Eukaryotic initiation factor 2alpha-independent pathway of stress granule induction by the natural product pateamine A. *J Biol Chem* **281**, 32870-8.

De Graeve, F., Debreuve, E., Rahmoun, S., Ecsedi, S., Bahri, A., Hubstenberger, A., Descombes, X. and Besse, F. (2019). Detecting and quantifying stress granules in tissues of multicellular organisms with the Obj.MPP analysis tool. *Traffic* **20**, 697-711.

Edwards, M. J., Walsh, D. A. and Li, Z. (1997). Hyperthermia, teratogenesis and the heat shock response in mammalian embryos in culture. *Int J Dev Biol* **41**, 345-58.

Fuse, Y., Nguyen, V. T. and Kobayashi, M. (2016). Nrf2-dependent protection against acute sodium arsenite toxicity in zebrafish. *Toxicol Appl Pharmacol* **305**, 136-142.

Gilks, N., Kedersha, N., Ayodele, M., Shen, L., Stoecklin, G., Dember, L. M. and Anderson, P.

(2004). Stress granule assembly is mediated by prion-like aggregation of TIA-1. *Mol Biol Cell* **15**, 5383-98.

Hetz, C. and Saxena, S. (2017). ER stress and the unfolded protein response in neurodegeneration. *Nat Rev Neurol* **13**, 477-491.

Icoglu Aksakal, F. and Ciltas, A. (2018). The impact of ultraviolet B (UV-B) radiation in combination with different temperatures in the early life stage of zebrafish (Danio rerio). *Photochem Photobiol Sci* **17**, 35-41.

Kedersha, N. and Anderson, P. (2007). Mammalian stress granules and processing bodies. *Methods Enzymol* **431**, 61-81.

Kedersha, N., Cho, M. R., Li, W., Yacono, P. W., Chen, S., Gilks, N., Golan, D. E. and Anderson, P. (2000). Dynamic shuttling of TIA-1 accompanies the recruitment of mRNA to mammalian stress granules. *J Cell Biol* **151**, 1257-68.

Kedersha, N., Ivanov, P. and Anderson, P. (2013). Stress granules and cell signaling: more than just a passing phase? *Trends Biochem Sci* **38**, 494-506.

Kedersha, N., Stoecklin, G., Ayodele, M., Yacono, P., Lykke-Andersen, J., Fritzler, M. J., Scheuner, D., Kaufman, R. J., Golan, D. E. and Anderson, P. (2005). Stress granules and processing bodies are dynamically linked sites of mRNP remodeling. *J Cell Biol* **169**, 871-84.

Kedersha, N., Tisdale, S., Hickman, T. and Anderson, P. (2008). Real-time and quantitative imaging of mammalian stress granules and processing bodies. *Methods Enzymol* **448**, 521-52.

Kedersha, N. L., Gupta, M., Li, W., Miller, I. and Anderson, P. (1999). RNA-binding proteins TIA-1 and TIAR link the phosphorylation of eIF-2 alpha to the assembly of mammalian stress granules. *J Cell Biol* **147**, 1431-42.

Kimmel, C. B. (1989). Genetics and early development of zebrafish. *Trends Genet* **5**, 283-8.

Kimmel, C. B., Ballard, W. W., Kimmel, S. R., Ullmann, B. and Schilling, T. F. (1995). Stages of embryonic development of the zebrafish. *Dev Dyn* **203**, 253-310.

Kimmel, C. B. and Warga, R. M. (1988). Cell lineage and developmental potential of cells in the zebrafish embryo. *Trends Genet* **4**, 68-74.

Li, J., Zhang, B. B., Ren, Y. G., Gu, S. Y., Xiang, Y. H. and Du, J. L. (2015). Intron targeting-mediated and endogenous gene integrity-maintaining knockin in zebrafish using the CRISPR/Cas9 system. *Cell Res* **25**, 634-7.

Li, Y. R., King, O. D., Shorter, J. and Gitler, A. D. (2013). Stress granules as crucibles of ALS pathogenesis. *J Cell Biol* **201**, 361-72.

Lodish, H. F. and Kong, N. (1993). The secretory pathway is normal in dithiothreitol-treated cells, but disulfide-bonded proteins are reduced and reversibly retained in the endoplasmic reticulum. *J Biol Chem* **268**, 20598-605.

Lowery, L. A. and Sive, H. (2005). Initial formation of zebrafish brain ventricles occurs independently of circulation and requires the nagie oko and snakehead/atp1a1a.1 gene products. *Development* **132**, 2057-67.

Mahboubi, H. and Stochaj, U. (2017). Cytoplasmic stress granules: Dynamic modulators of cell signaling and disease. *Biochim Biophys Acta Mol Basis Dis* **1863**, 884-895.

Marrone, L., Poser, I., Casci, I., Japtok, J., Reinhardt, P., Janosch, A., Andree, C., Lee, H. O., Moebius, C., Koerner, E. et al. (2018). Isogenic FUS-eGFP iPSC Reporter Lines Enable Quantification of FUS Stress Granule Pathology that Is Rescued by Drugs Inducing Autophagy. *Stem Cell Reports* **10**, 375-389.

Martin, S. and Tazi, J. (2014). Visualization of G3BP stress granules dynamics in live primary cells. *J Vis Exp*.

Matsuki, H., Takahashi, M., Higuchi, M., Makokha, G. N., Oie, M. and Fujii, M. (2013). Both G3BP1 and G3BP2 contribute to stress granule formation. *Genes Cells* **18**, 135-46.

Maziuk, B., Ballance, H. I. and Wolozin, B. (2017). Dysregulation of RNA Binding Protein Aggregation in Neurodegenerative Disorders. *Front Mol Neurosci* **10**, 89.

McCollum, C. W., Hans, C., Shah, S., Merchant, F. A., Gustafsson, J. A. and Bondesson, M. (2014). Embryonic exposure to sodium arsenite perturbs vascular development in zebrafish. *Aquat Toxicol* **152**, 152-63.

McCormick, C. and Khaperskyy, D. A. (2017). Translation inhibition and stress granules in the antiviral immune response. *Nat Rev Immunol* **17**, 647-660.

Menon, T. and Nair, S. (2018). Transient window of resilience during early development minimizes teratogenic effects of heat in zebrafish embryos. *Dev Dyn* **247**, 992-1004.

Mishra, S., Wu, S. Y., Fuller, A. W., Wang, Z., Rose, K. L., Schey, K. L. and McHaourab, H. S. (2018). Loss of alphaB-crystallin function in zebrafish reveals critical roles in the development of the lens and stress resistance of the heart. *J Biol Chem* **293**, 740-753.

Mokas, S., Mills, J. R., Garreau, C., Fournier, M. J., Robert, F., Arya, P., Kaufman, R. J., Pelletier, J. and Mazroui, R. (2009). Uncoupling stress granule assembly and translation initiation inhibition. *Mol Biol Cell* **20**, 2673-83.

Mu, Y., Li, X. Q., Zhang, B. and Du, J. L. (2012). Visual input modulates audiomotor function via hypothalamic dopaminergic neurons through a cooperative mechanism. *Neuron* **75**, 688-99.

Naidoo, N. (2009). The endoplasmic reticulum stress response and aging. *Rev Neurosci* **20**, 23-

37.

Nover, L., Scharf, K. D. and Neumann, D. (1989). Cytoplasmic heat shock granules are formed from precursor particles and are associated with a specific set of mRNAs. *Mol Cell Biol* **9**, 1298-308.

Oakes, S. A. and Papa, F. R. (2015). The role of endoplasmic reticulum stress in human pathology. *Annu Rev Pathol* **10**, 173-94.

Paix, A., Folkmann, A., Goldman, D. H., Kulaga, H., Grzelak, M. J., Rasoloson, D., Paidemarry, S., Green, R., Reed, R. R. and Seydoux, G. (2017). Precision genome editing using synthesis-dependent repair of Cas9-induced DNA breaks. *Proc Natl Acad Sci U S A* **114**, E10745-E10754.

Parker, F., Maurier, F., Delumeau, I., Duchesne, M., Faucher, D., Debussche, L., Dugue, A., Schweighoffer, F. and Tocque, B. (1996). A Ras-GTPase-activating protein SH3-domain-binding protein. *Mol Cell Biol* **16**, 2561-9.

Protter, D. S. W. and Parker, R. (2016). Principles and Properties of Stress Granules. *Trends Cell Biol* **26**, 668-679.

Shelkovnikova, T. A., Dimasi, P., Kukharsky, M. S., An, H., Quintiero, A., Schirmer, C., Buee, L., Galas, M. C. and Buchman, V. L. (2017). Chronically stressed or stress-preconditioned neurons fail to maintain stress granule assembly. *Cell Death Dis* **8**, e2788.

Shen, J., Chen, X., Hendershot, L. and Prywes, R. (2002). ER stress regulation of ATF6 localization by dissociation of BiP/GRP78 binding and unmasking of Golgi localization signals. *Dev Cell* **3**, 99-111.

Solnica-Krezel, L., Stemple, D. L. and Driever, W. (1995). Transparent things: cell fates and cell movements during early embryogenesis of zebrafish. *Bioessays* **17**, 931-9.

Spitsbergen, J. M. and Kent, M. L. (2003). The state of the art of the zebrafish model for toxicology

and toxicologic pathology research--advantages and current limitations. *Toxicol Pathol* **31 Suppl**, 62-87.

Tourriere, H., Chebli, K., Zekri, L., Courselaud, B., Blanchard, J. M., Bertrand, E. and Tazi, J. (2003). The RasGAP-associated endoribonuclease G3BP assembles stress granules. *J Cell Biol* **160**, 823-31.

Tsai, W. C., Gayatri, S., Reineke, L. C., Sbardella, G., Bedford, M. T. and Lloyd, R. E. (2016). Arginine Demethylation of G3BP1 Promotes Stress Granule Assembly. *J Biol Chem* **291**, 22671-22685.

van der Laan, A. M., van Gemert, A. M., Dirks, R. W., Noordermeer, J. N., Fradkin, L. G., Tanke, H. J. and Jost, C. R. (2012). mRNA cycles through hypoxia-induced stress granules in live Drosophila embryonic muscles. *Int J Dev Biol* **56**, 701-9.

Vognsen, T., Moller, I. R. and Kristensen, O. (2011). Purification, crystallization and preliminary X-ray diffraction of the G3BP1 NTF2-like domain. *Acta Crystallogr Sect F Struct Biol Cryst Commun* **67**, 48-50.

Vognsen, T., Moller, I. R. and Kristensen, O. (2013). Crystal structures of the human G3BP1 NTF2-like domain visualize FxFG Nup repeat specificity. *PLoS One* **8**, e80947.

Walsh, D. A., Edwards Mj, M. J. and Smith, M. S. R. (1997). Heat shock proteins and their role in early mammalian development. *Experimental & Molecular Medicine* **29**, 139-150.

Wang, R., Jiang, X., Bao, P., Qin, M. and Xu, J. (2019). Circadian control of stress granules by oscillating EIF2alpha. *Cell Death Dis* **10**, 215.

Wheeler, J. R., Matheny, T., Jain, S., Abrisch, R. and Parker, R. (2016). Distinct stages in stress granule assembly and disassembly. *Elife* **5**.

White, J. P. and Lloyd, R. E. (2012). Regulation of stress granules in virus systems. *Trends*

Microbiol **20**, 175-83.

Wolozin, B. (2012). Regulated protein aggregation: stress granules and neurodegeneration. *Mol Neurodegener* **7**, 56.

Xu, W., Bao, P., Jiang, X., Wang, H., Qin, M., Wang, R., Wang, T., Yang, Y., Lorenzini, I., Liao, L. et al. (2019). Reactivation of nonsense-mediated mRNA decay protects against C9orf72 dipeptide-repeat neurotoxicity. *Brain* **142**, 1349-1364.

Zampedri, C., Tinoco-Cuellar, M., Carrillo-Rosas, S., Diaz-Tellez, A., Ramos-Balderas, J. L., Pelegri, F. and Maldonado, E. (2016). Zebrafish P54 RNA helicases are cytoplasmic granule residents that are required for development and stress resilience. *Biol Open* **5**, 1473-1484.

Figures

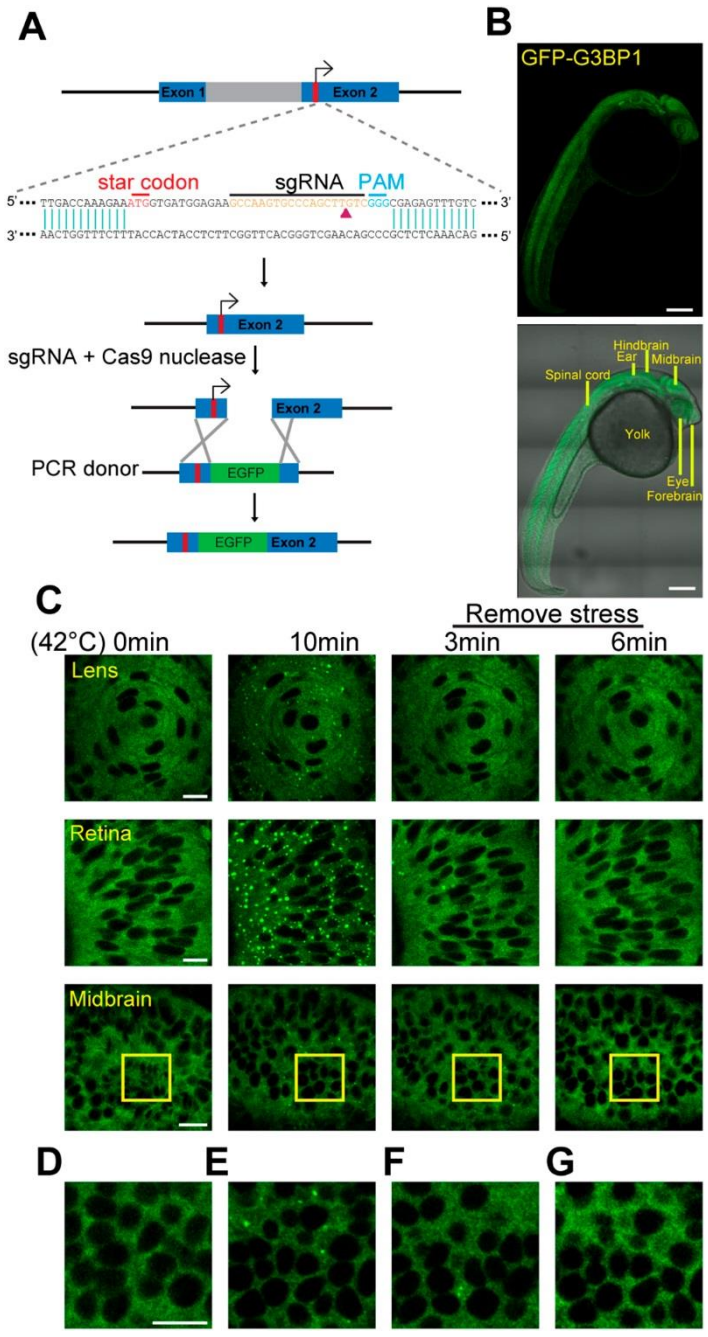

Fig. 1. Establishment and characterization of GFP-G3BP1 knockin zebrafish

(A)Schematic representation of the gene editing strategy used to insert GFP into the zebrafish G3BP1 locus. (B) Top: A Z-stacked picture showing the expression pattern of GFP-G3BP1 in 1dpf fish under basal condition. Bottom: A picture showing the GFP reporter signal overlapped

with bright-field image (Scale bar =200μm). (C) Stress granules in lens, retina and midbrain cells of 1dpf GFP-G3BP1 KI zebrafish when exposed to 42°C for 0 or 10min, and at 3 and 6 minutes after the removal of heat stress shock. (D-G) Enlarged image of the yellow square areas in the midbrain region in the pictures above (C). (Scale bar =10μm)

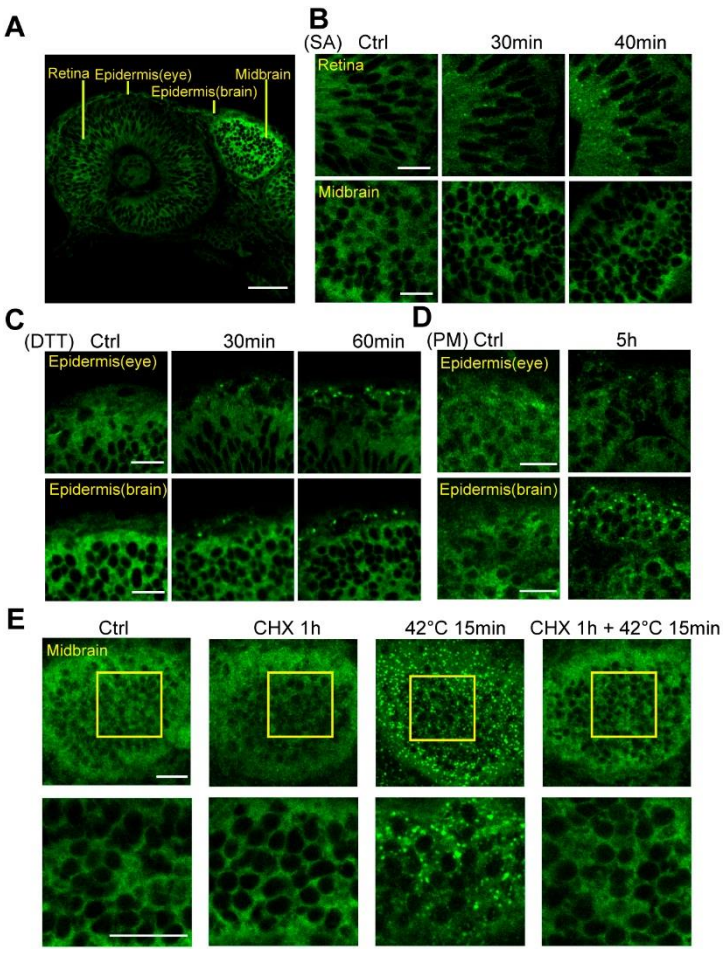

Fig. 2. The GFP-G3BP1 reporter responds to oxidative and ER stresses in zebrafish

(A)A single layer image showing the GPF-G3BP1 expression under basal condition and the region examined in (B) and (C). (B) Induction of stress granules in the retina, but not in the brain, of 1dpf GFP-G3BP1 KI zebrafish after 30mM sodium arsenite (SA) exposure in the medium for indicated amount of time. (C) Induction of stress granules in the epidermal cells in fish exposed to 20mM Dithiothreitol (DTT) stress for indicated amount of time. (D) Induction of stress granules in the epidermal cells in fish exposed to 10mg/ml Puromycin (PM) stress for 5h. (E) Stress granule formation in midbrain was suppressed by 10mg/ml Cycloheximide (CHX). Enlarged image of the yellow square areas in the midbrain region was shown beneath. Images represented similar results from 2-3 independent experiments each with 3-4 zebrafish examined at each condition. (Scale bar =20μm)

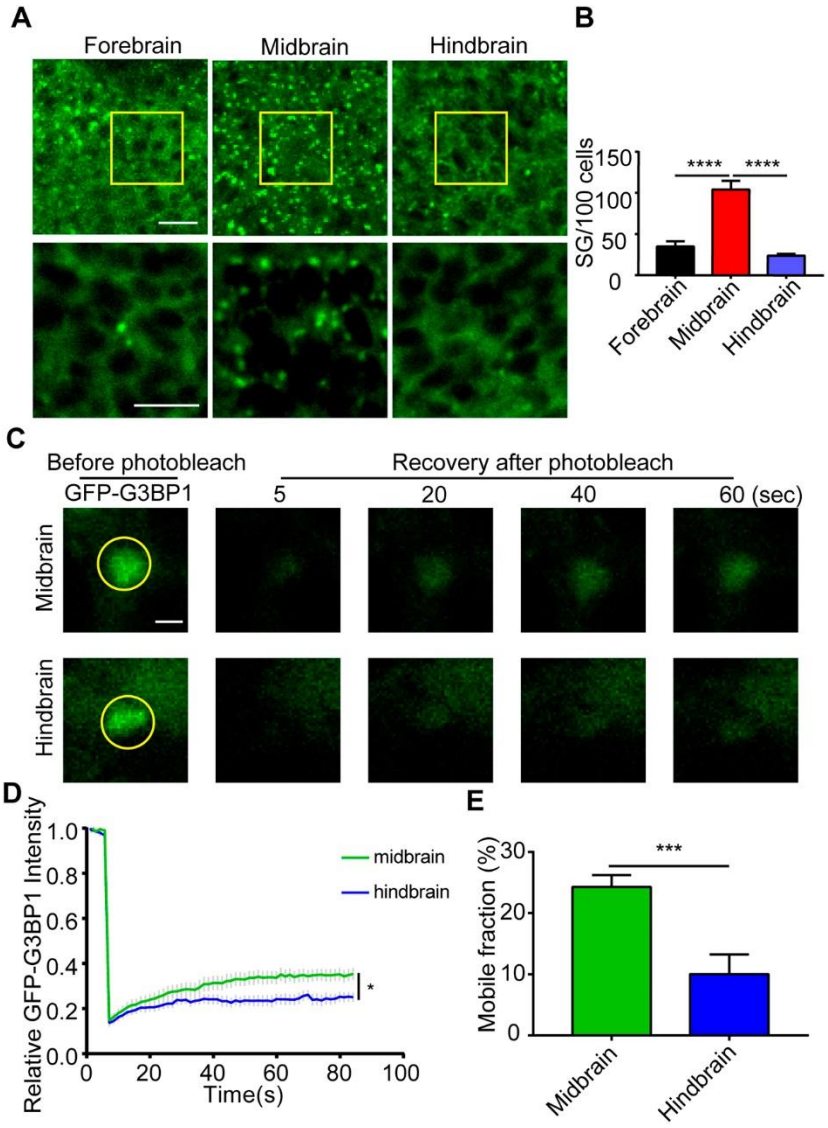

Fig. 3. Stress granule formation varies by different brain regions

(A) Ten-minute heat shock-induced stress granules in the forebrain, midbrain, and hindbrain region in 1dpf GFP-G3BP1 KI zebrafish. The yellow-boxed areas were enlarged and shown in the lower panels (Scale bar =10μm). (B) Quantification of stress granules (sized≥0.1μm) formed in cells from each region. Cells quantified were at the same depth (20μm under the epidermis) in each region to minimize the potential difference due to heat conductance. Values represent mean ± S.E.M.; n = 5 zebrafish, 100-120 cells per field. ****P ≤ 0.0001 by unpaired Student's-t-test). (C-E) Stress granule dynamics in heat-shocked cells from midbrain and hindbrain in 1dpf GFP-G3BP1 KI zebrafish. After removal of heat shock, selected stress

granules were analyzed by FRAP. All the stress granule-positive cells analyzed by FRAP were at the same depth (10μm under epidermis). Representative images of the stress granules before and after photobleaching at different time were shown in (C), with the signal intensity of GFP fluorescence from FRAP shown in (D). The average fluorescence intensity before photobleaching was designated as 1. The mobile fraction calculated from the FRAP analysis in was shown in (E) (Scale bar =2μm). Values represent mean ± S.E.M.; for each brain region, 14-15 cells from 5-6 zebrafish were analyzed. **P ≤ 0.01, ***P ≤0.001 by unpaired Student's-t-test.

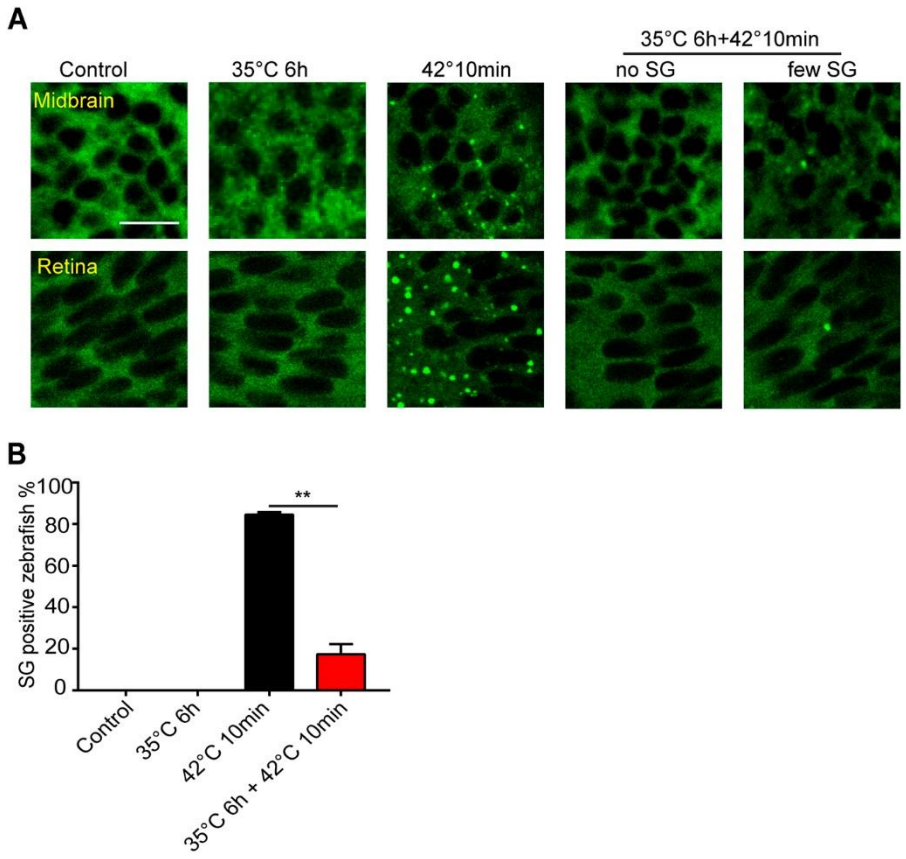

Fig. 4. Heat pre-conditioning suppresses stress granule formation

(A)Representative images showing stress granule formation in midbrain and retina cells of 1dpf GFP-G3BP1 KI zebrafish with indicated treatment paradigms. Control: fish kept at ambient temperature 28 ºC; 35ºC 6h: fish kept at 35ºC for 6h; 42ºC 10 min: fish heat-shocked at 42ºC for 10 min; 35ºC for 6h+42ºC 10 min: fish first exposed to 35ºC for 6h, then heat shocked for 10 min at 42ºC. (Scale bar =10μm) (B) The quantification showing the percentage of zebrafish with stress granules in the midbrain. Values represent mean ± S.E.M.; n=2 independent experiments, with n=10, 7, 19 and 17 fish for each condition. **$P \leq 0.01$, by unpaired Student's-t-test.

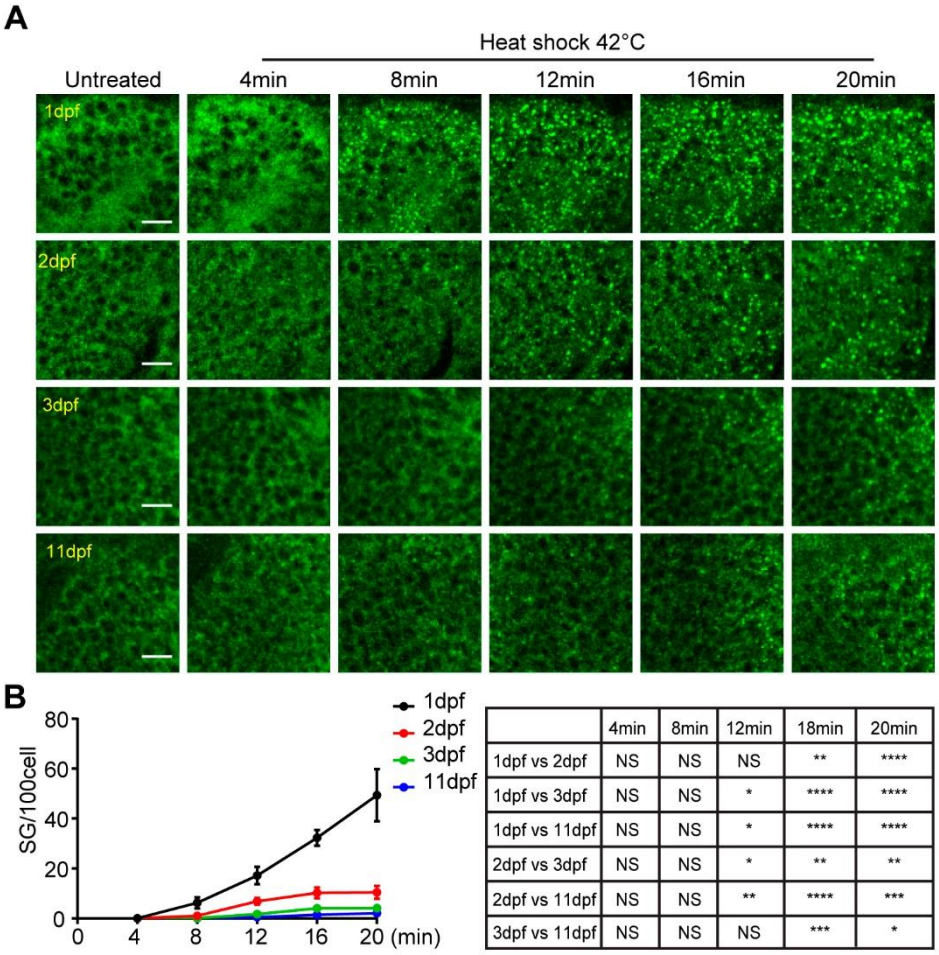

	4min	8min	12min	18min	20min
1dpf vs 2dpf	NS	NS	NS	**	****
1dpf vs 3dpf	NS	NS	*	****	****
1dpf vs 11dpf	NS	NS	*	****	****
2dpf vs 3dpf	NS	NS	*	**	**
2dpf vs 11dpf	NS	NS	**	****	***
3dpf vs 11dpf	NS	NS	NS	***	*

Fig.5. Delayed stress granule formation in zebrafish larvae

(A)Representative images showing the formation of stress granules in the midbrain (optical tectum) at indicated time with heat shock a 42°C for GFP-G3BP1 KI fish with different age during early development.(B) Quantification of the number of stress granules (sized ≥1μm) at the same depth (20μm under epidermis) in fish from 1 to 11 dpf as indicated. Statistical results analyzed by two-way ANOVA followed by multiple comparison were showed in the table at right side (mean ± S.E.M.; n = 4 zebrafish for each age, with 100-300 cells scored for each fish. **P ≤ 0.05, **P ≤ 0.01, ***P ≤0.001, ***P ≤0.0001)

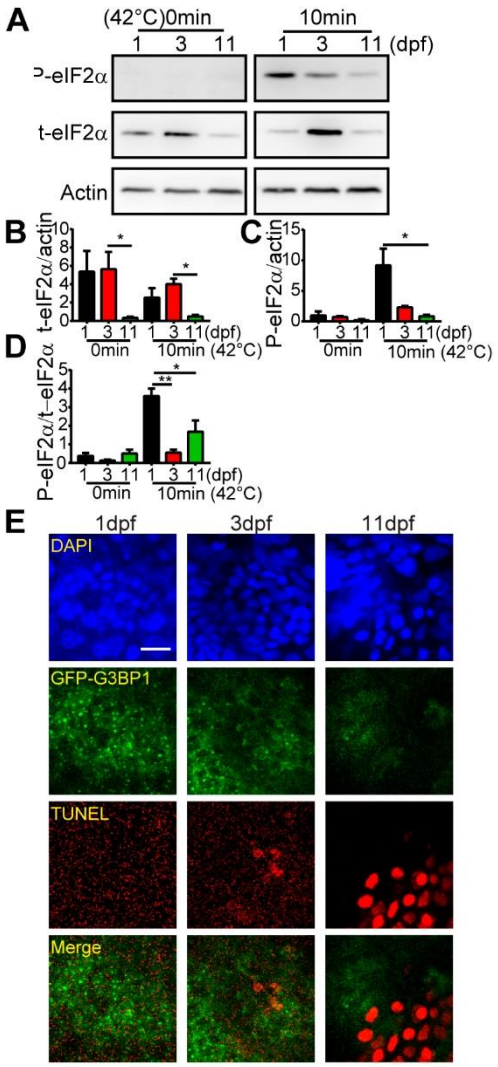

Fig. 6. Heat shock-induced cell death coincides with decreased level of P-eIF2α and reduced number of stress granules in fish larvae

(A) Representative western blots showing the expression of p-eIF2α, t-eIF2α and actin after 10 min heat shock in the brain of 1, 3, 11 dpf GFP-G3BP1 KI zebrafish. Quantification of the relative expression of indicated proteins was presented in (B)-(D). Values represent mean ± S.E.M.; n = 3 independent experiments, for each condition, 15-20 zebrafish brains were pooled for protein analysis. *P ≤ 0.05, **P ≤ 0.01, by unpaired Student's-t-test) (E) Representative images showing the stress granule formation and cell death (revealed by TUNEL) in the epidermis of 1, 3, 11dpf GFP-G3BP1 KI zebrafish exposed to 42°C for 20min (n = 4-5 zebrafish at each age with similar results). (Scale bar =10μm)

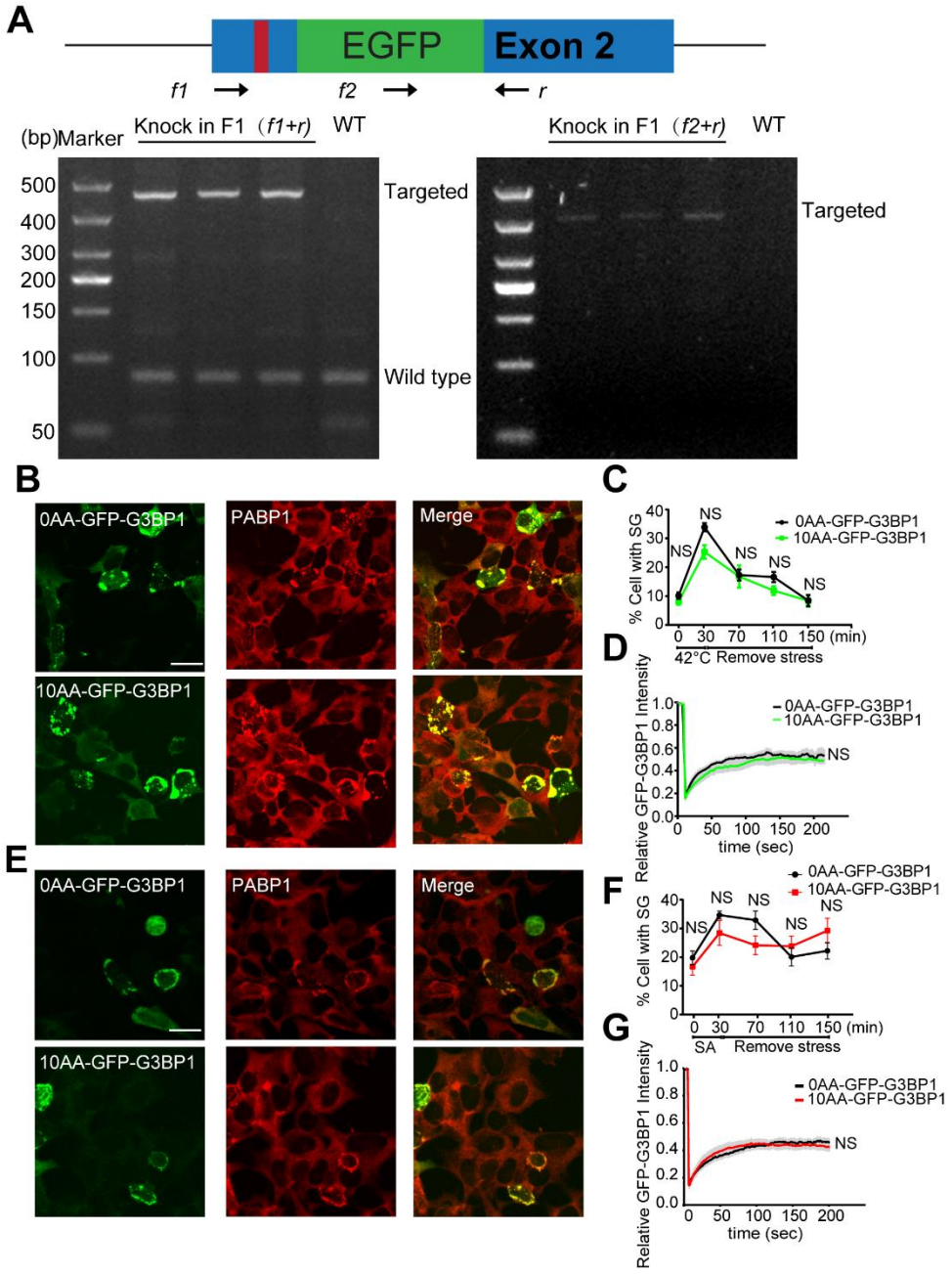

Fig S1. Validation of GFP-G3BP1 KI zebrafish

(A)Genotyping strategy and results from two sets of primers (*f1+r and f2+r*).

(B) Representative images showing the same response of 0AA-GFP-G3BP1 or 10AA-GFP-G3BP1 to heat shock stress (42°C for 30 minutes) in SH-SY5Y cells. (C) Stress granule formation in SH-SY5Y cells transfected with either 0AA-GFP-G3BP1 or

10AA-GFP-G3BP1 reporter plasmid after heat shock at 42°C for 30 minutes. Cells were fixed and immunolabeled at indicated time after removal of stress for stress granule imaging and quantification (mean ± S.E.M.; n=10 fields for each time point, at least 10-15 GFP positive cells per field. (D) FRAP analysis of heat shocked SH-SY5Y cells expressing 0AA-GFP-G3BP1 or 10AA-GFP-G3BP1. Cells were heat shocked at 42°C for 30 minutes, and the stress granules dynamics were analyzed by FRAP after stress removal (mean ± S.E.M.; n = 7-8 cells per sample, by unpaired Student's-*t*-test). (E) Representative images showing the same response of 0AA-GFP-G3BP1 or 10AA-GFP-G3BP1 to sodium arsenite stress (20μM for 30 minutes) in SH-SY5Y cells. (F) SH-SY5Y cells transfected with either reporter plasmid were stress shocked with 20μM sodium arsenite for 30 minutes and fixed at indicated time after removal of stress for stress granule imaging and quantification (mean ± S.E.M.; n=10 fields for each time point, at least 10-15 GFP positive cells per field. (G) FRAP analysis of SH-SY5Y cells expressing 0AA-GFP-G3BP1 or 10AA-GFP-G3BP1. Cells were treated SA as described above. After stress was removed, stress granules dynamics were analyzed by FRAP. For FRAP the average fluorescence before photobleaching was designated as 1 (mean ± S.E.M.; n = 8-9 cells per sample, by unpaired Student's-*t*-test). (Scale bar =10μm)

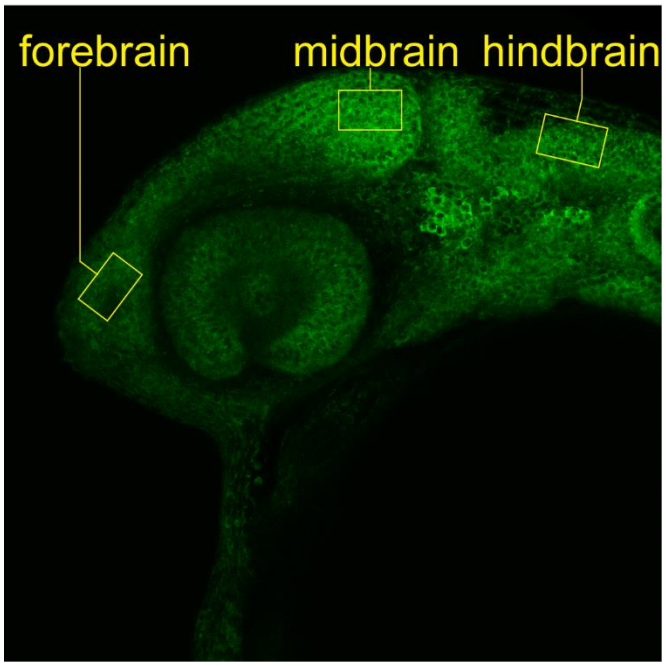

Fig S2. The forebrain, midbrain, hindbrain regions in 1dpf fish embryo selected for SG formation and dynamics analysis. 1dpf zebrafish at normal condition was fixed in 4% PFA for imaging.

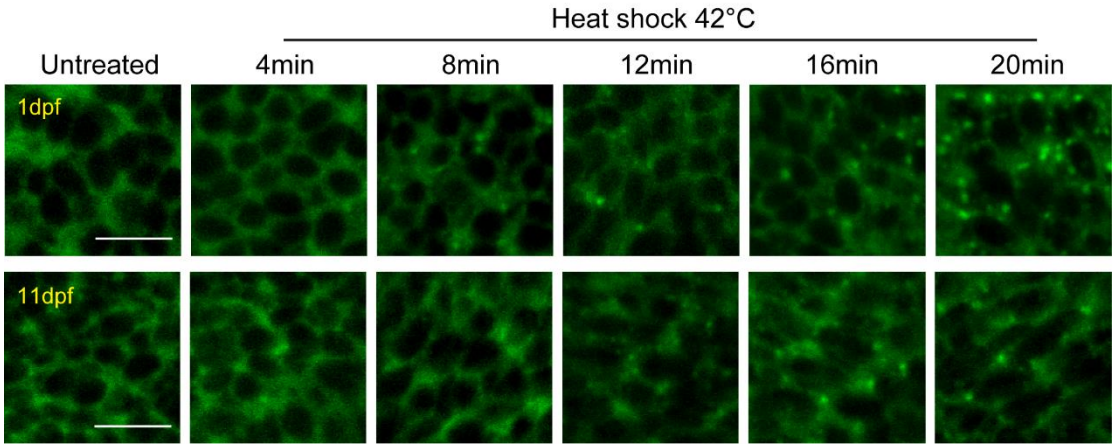

Fig S3. Delayed stress granule formation in zebrafish larvae

Enlarged images of the midbrain region of 1dpf and 11dpf zebrafish at various time points after heat shock as shown in Fig 5A. Scale bar =10μm

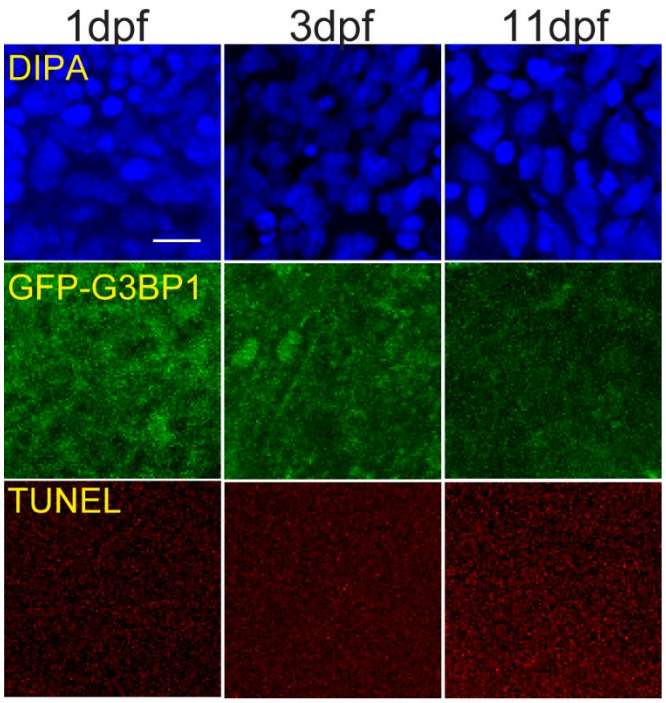

Fig S4. Absence of cell death in zebrafish kept at ambient condition. Zebrafish of different age kept at 28 ºC were fixed in 4% PFA for TUNEL assay.

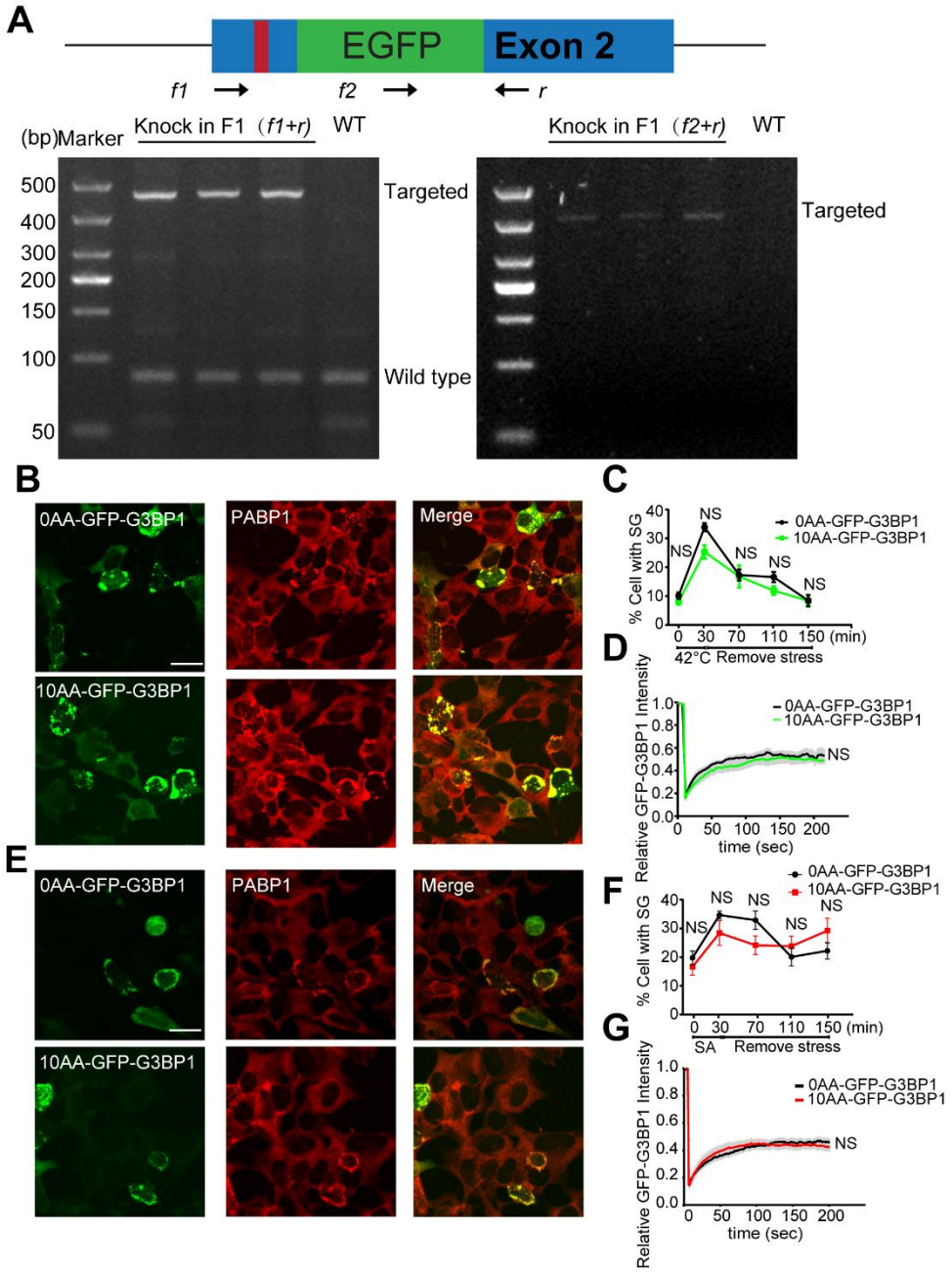

Fig S1. Validation of GFP-G3BP1 KI zebrafish

(A)Genotyping strategy and results from two sets of primers (*f1+r and f2+r*).

(B) Representative images showing the same response of 0AA-GFP-G3BP1 or 10AA-GFP-G3BP1 to heat shock stress (42°C for 30 minutes) in SH-SY5Y cells. (C) Stress granule formation in SH-SY5Y cells transfected with either 0AA-GFP-G3BP1 or

10AA-GFP-G3BP1 reporter plasmid after heat shock at 42°C for 30 minutes. Cells were fixed and immunolabeled at indicated time after removal of stress for stress granule imaging and quantification (mean ± S.E.M.; n=10 fields for each time point, at least 10-15 GFP positive cells per field. (D) FRAP analysis of heat shocked SH-SY5Y cells expressing 0AA-GFP-G3BP1 or 10AA-GFP-G3BP1. Cells were heat shocked at 42°C for 30 minutes, and the stress granules dynamics were analyzed by FRAP after stress removal (mean ± S.E.M.; n = 7-8 cells per sample, by unpaired Student's-*t*-test). (E) Representative images showing the same response of 0AA-GFP-G3BP1 or 10AA-GFP-G3BP1 to sodium arsenite stress (20μM for 30 minutes) in SH-SY5Y cells. (F) SH-SY5Y cells transfected with either reporter plasmid were stress shocked with 20μM sodium arsenite for 30 minutes and fixed at indicated time after removal of stress for stress granule imaging and quantification (mean ± S.E.M.; n=10 fields for each time point, at least 10-15 GFP positive cells per field. (G) FRAP analysis of SH-SY5Y cells expressing 0AA-GFP-G3BP1 or 10AA-GFP-G3BP1. Cells were treated SA as described above. After stress was removed, stress granules dynamics were analyzed by FRAP. For FRAP the average fluorescence before photobleaching was designated as 1 (mean ± S.E.M.; n = 8-9 cells per sample, by unpaired Student's-*t*-test). (Scale bar =10μm)

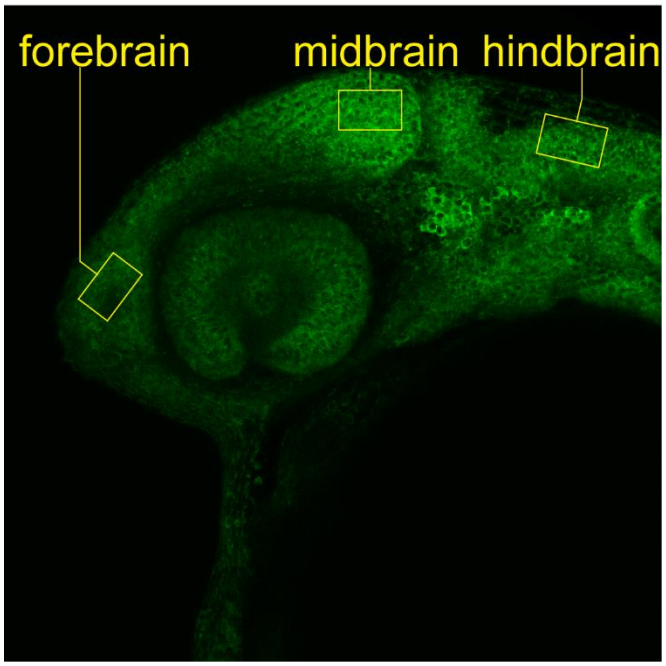

Fig S2. The forebrain, midbrain, hindbrain regions in 1dpf fish embryo selected for SG formation and dynamics analysis. 1dpf zebrafish at normal condition was fixed in 4% PFA for imaging.

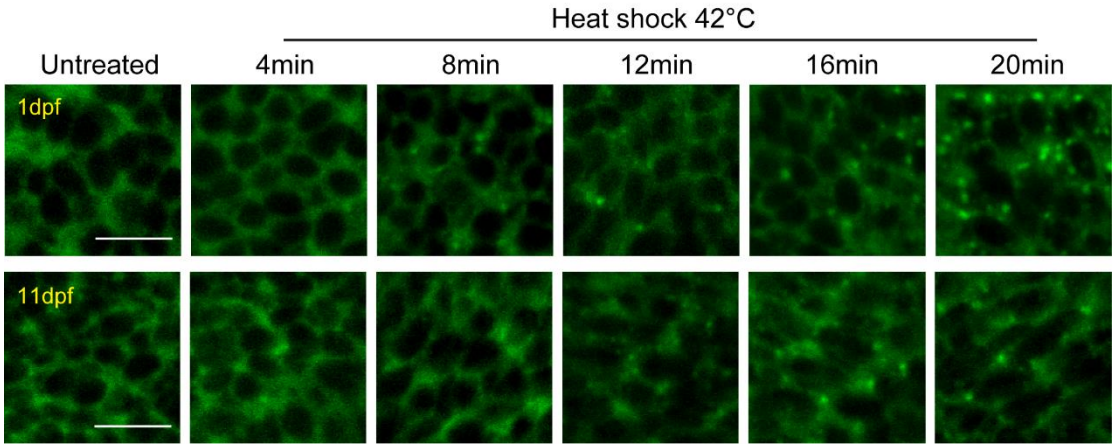

Fig S3. Delayed stress granule formation in zebrafish larvae

Enlarged images of the midbrain region of 1dpf and 11dpf zebrafish at various time points after heat shock as shown in Fig 5A. Scale bar =10μm

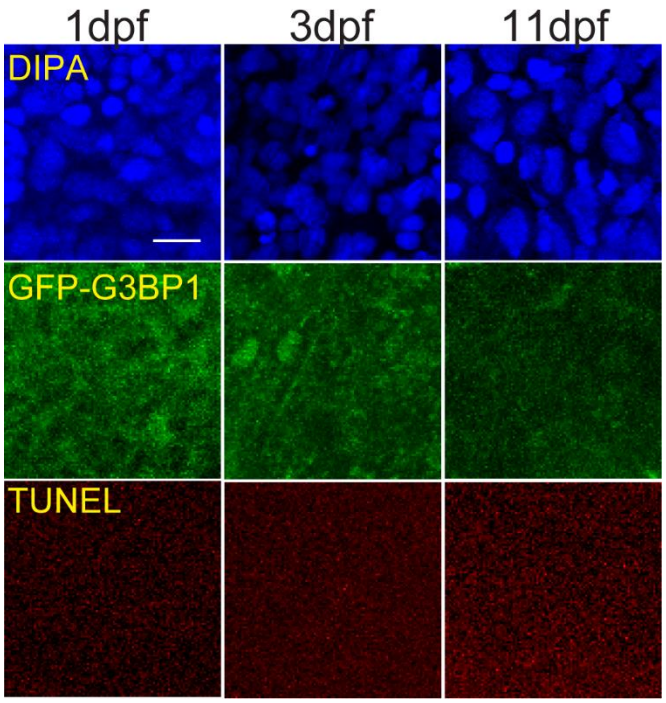

Fig S4. Absence of cell death in zebrafish kept at ambient condition. Zebrafish of different age kept at 28 ºC were fixed in 4% PFA for TUNEL assay.